

# Bioactivities and Anti-Cancer Activities of NKT-Stimulatory Phenyl-Glycolipid Formulated with a PEGylated Lipid Nanocarrier

Jung-Tung Hung<sup>1</sup>, Shih-Pin Chiou<sup>1</sup>, Yun-Hsin Tang<sup>1-3</sup>, Jing-Rong Huang<sup>1</sup>, Fei-Yun Lo<sup>1</sup>, Alice L Yu<sup>1,4</sup>

<sup>1</sup>Institute of Stem Cell and Translational Cancer Research, Chang Gung Memorial Hospital at Linkou, Taoyuan, Taiwan; <sup>2</sup>Department of Obstetrics and Gynecology, Chang Gung Memorial Hospital, Linkou Branch, and Chang Gung University, College of Medicine, Taoyuan, Taiwan; <sup>3</sup>Gynecologic Cancer Research Center, Chang Gung Memorial Hospital, Linkou Branch, Taoyuan, Taiwan; <sup>4</sup>Department of Pediatrics, University of California in San Diego, San Diego, California, USA

Correspondence: Alice L Yu, Institute of Stem Cell and Translational Cancer Research, Chang Gung Memorial Hospital at Linkou, No. 15, Wenhua 1st Road, Guishan District, Taoyuan City, 333, Taiwan, Tel +886 3 328 1200#7813, Email alyu@health.ucsd.edu

**Purpose:** The glycolipid  $\alpha$ -galactosylceramide ( $\alpha$ -GalCer), when presented by CD1d, can modulate the immune system through the activation of natural killer T (NKT) cells. Previously, we synthesized over 30 analogs of  $\alpha$ -GalCer and identified a compound, C34, which features two phenyl rings on the acyl chain. C34 exhibited the most potent NKT-stimulating activities, characterized by strong Th1-biased cytokines and potent anti-tumor effects in several murine tumor models. Importantly, unlike  $\alpha$ -GalCer, C34 did not induce NKT cell anergy. Despite these promising results, the clinical application of C34 is limited by its poor aqueous solubility. PEGylation enhances the solubility of hydrophobic drugs, and numerous PEGylated drugs have received clinical approval. Consequently, we assessed the biological activity of PEGylated C34 in this study.

**Methods:** Murine NK1.2 cells were cultured with A20-CD1d cells in the presence of either PEGylated lipid nanocarriers encapsulating C34 (PLN-C34) or C34 dissolved in DMSO to determine IL-2 production via ELISA. C57BL/6 mice were i.v. injected with C34 or PLN-C34 to examine cytokine profiles and immune cell populations using luminex and flow cytometry, respectively. The anticancer effects of C34 and PLN-C34 were evaluated in mice bearing TC-1 lung cancer and B16 melanoma tumors. Additionally, human PBMCs were cultured with C34 or PLN-C34 to measure cytokine production through luminex.

**Results:** PLN-C34 demonstrated a comparable capacity to C34 in activating the NKT cell line in vitro and inducing various cytokines in vivo. Furthermore, treatment with either PLN-C34 or C34 significantly prolonged the survival of TC-1- and B16F10-bearing mice to a similar extent. Additionally, PLN-C34 effectively stimulated cytokine responses in human NKT cells, comparable to those induced by C34.

**Conclusion:** These findings demonstrate that the newly formulated PLN-C34 retains NKT-stimulatory activity and anti-cancer efficacy of C34, supporting the potential of PLN as a solvent for C34 for further development in cancer therapy.

**Keywords:** phenyl-glycolipid, NKT cells, PEGylated lipid nanocarrier, anti-cancer

## Introduction

Natural killer T (NKT) cells represent a small subset of T lymphocytes that express T cell receptors (TCR) and NK cell markers. The TCR of NKT cells recognizes the glycolipid molecule  $\alpha$ -galactosylceramide ( $\alpha$ -GalCer), which is presented by CD1d on antigen-presenting cells and epithelial cells.<sup>1</sup> The CD1d-restricted NKT cells harbor a unique invariant TCR. The engagement of this invariant TCR with CD1d-presented  $\alpha$ -GalCer triggers the rapid secretion of both Th1 and Th2 cytokines by NKT cells.<sup>2-4</sup> In view of their potent immunomodulatory functions, NKT cells have been exploited for their potential in preventing tumor metastases,<sup>5</sup> reducing tumor growth, inhibiting bacterial or viral infections, and ameliorating the progression of autoimmune diseases in mouse models.<sup>6-9</sup> However,  $\alpha$ -GalCer can upregulate PD1 and cbl-b in NKT cells, inducing NKT cell anergy because of the low-avidity engagement with TCR.<sup>10</sup> Repeated administration of  $\alpha$ -GalCer in mice also increased immunosuppressive myeloid-derived suppressor cells (MDSCs) in the spleen.<sup>10</sup> Moreover,

$\alpha$ -GalCer elicits strong production of both Th1 and Th2 cytokines.<sup>11</sup> Although the Th1 response is crucial for anti-tumor immunity, the Th2 response has traditionally been seen as favoring tumor growth. Such properties may explain the limited anti-cancer efficacy of  $\alpha$ -GalCer in early clinical trials.<sup>12,13</sup> Therefore, various structural modifications of  $\alpha$ -GalCer have been developed to manipulate immune polarization of NKT cells.<sup>14</sup> For instance, adding phenyl groups to the acyl chain of glycolipids stimulates a Th1-biased immune response,<sup>15,16</sup> while shortening the sphingosine chain length triggers a Th2-biased immune response.<sup>17</sup> We previously evaluated the biological activity of  $\alpha$ -GalCer analogs, using an *in vitro* assay to determine cytokine production from NKT cells upon stimulation by CD1d-presented  $\alpha$ -GalCer analogs.<sup>15,18</sup> We found that C34, a glycolipid containing two phenyl rings on the acyl chain, elicits the most potent Th1-biased immunity among a variety of  $\alpha$ -GalCer derivatives. *In vivo*, C34 stimulates mouse NKT cells to secrete higher levels of Th1 cytokines, such as IFN- $\gamma$  and IL-2. It also exhibits greater anti-tumor activity than  $\alpha$ -GalCer and other phenyl glycolipids in syngeneic murine tumor models of TC-1 lung cancer and B16F10 melanoma.<sup>15</sup> These effects of C34 are attributed to the high binding affinity and stability of C34-CD1d complex with the TCR of NKT cells. More importantly, unlike  $\alpha$ -GalCer, C34 neither induces anergy of NKT cells nor increases accumulation of MDSCs in TC-1-bearing mice upon multi-dose administration,<sup>10</sup> further supporting the use of C34 as an anticancer therapeutic.

All the aforementioned studies were performed using dimethyl sulfoxide (DMSO) as a solvent because C34 is hydrophobic and difficult to dissolve in water. In preclinical studies, DMSO is predominately used as a solvent for hydrophobic agents. However, the clinical use of DMSO is limited to the treatment of interstitial cystitis via intravesical injection. Moreover, DMSO has been reported to cause oxidative stress and induce embryonic defects in mouse preimplantation embryos.<sup>19</sup> In rats, DMSO could induce retinal apoptosis at low concentrations.<sup>20</sup> Since DMSO is not suitable for systemic administration, developing an appropriate formulation for C34 is crucial to facilitate its clinical pharmaceutical applications.

The water solubility of a drug is crucial for its design and development. Poorly water-soluble agents often suffer from poor absorption and limited bioactivity. To address this issue, hydrophobic agents are commonly mixed with surfactants, amphiphilic block copolymers, or lipids, to form micelles, disk-like micelles, vesicles, and bilayers in water, thereby facilitating their delivery.<sup>21–23</sup> Polyethylene glycol (PEG) offers many favorable properties for drug delivery, including biocompatibility, low toxicity, and ease of excretion.<sup>24,25</sup> PEGylated lipids can self-assemble into core-shell nanostructures in aqueous solution, enhancing the solubility of hydrophobic drugs.<sup>26</sup> For example, sterically stabilized micelles (SSMs), a type of PEG-based nanocarrier, possess a hydrophobic core and an ionic interface capable of associating with a variety of poorly soluble therapeutic and diagnostic agents.<sup>27</sup> However, it remains unclear whether a PEG-based nanocarrier can increase the solubility and maintain biological function of the glycolipid C34.

In the present study, we have demonstrated that PEGylated lipid-based nanocarriers (PLN) mixed with hydrophobic phenyl glycolipid C34 (PLN-C34) were able to activate NKT cells *in vitro* and displayed comparable bioactivity to C34 in DMSO *in vivo*.

## Materials and Methods

### Cell Lines and Reagents

mNK1.2 and A20-CD1d cells were kindly provided by Dr. Mitchell Kronenberg. Mouse lung cancer TC-1 and mouse melanoma B16F10 cells were obtained from ATCC. The TC-1, mNK1.2, and A20-CD1d cells were maintained in RPMI-1640, while B16F10 cells were maintained in DMEM medium. Both media were supplemented with 10% heat-inactivated fetal bovine serum, 100  $\mu$ g/mL streptomycin, and 100  $\mu$ g/mL penicillin (Invitrogen, Frederick, MD).

C34 and PEGylated lipid nanocarrier-encapsulated C34 (PLN-C34) were kindly provided by OPKO Health Inc. C34 was dissolved in 100% DMSO at a concentration of 2 mg/mL. PLN is a proprietary formulation by OPKO Company. The production of PLN-C34 utilized a phospholipid polymer DSPE-mPEG2000 (1,2-Distearoyl-sn-glycero-3-phosphoethanolamine-N-[methoxy(polyethylene glycol)-2000]), which is a biocompatible, biodegradable amphiphilic material. Since DSPE-mPEG2000 contains both hydrophobic and hydrophilic regions, it can form micelles with a neutral charge. The PLN-C34's size is around 20–30 nm. To sterilize the solution, PLN-C34 was syringe-filtered using a 0.22  $\mu$ m PVDF filter. The sample was then diluted 10-fold in methanol, and the C34 content was quantified by HPLC. PLN-C34 was

dissolved in double-distilled water at 1 mg/mL. Immediately before in vivo administration, all glycolipids were diluted in PBS.

## Evaluation of in vitro Effect of C34 and PLN-C34 Using A20-CD1d and mNK1.2 Cells

A20-CD1d cells ( $10^4/50 \mu\text{L}$ ) and mNK1.2 cells ( $10^4/50 \mu\text{L}$ ) were seeded into each well of a 96-well plate. C34 in DMSO (abbreviated as C34) and PLN-C34 were diluted to a concentration of 10  $\mu\text{g/mL}$  in complete RPMI-1640 medium. Ten microliters of the diluted C34 and PLN-C34 were added to each well containing the A20-CD1d/mNK1.2 cells and incubated at 37°C. After 3, 6, and 24 hours, the culture medium was collected to determine the level of IL-2 by ELISA.

## Enzyme-Linked Immunosorbent Assay (ELISA) for Mouse IL-2

The concentration of mIL-2 was determined using the Mouse IL-2 DuoSet ELISA kit (DY402, R&D, USA). Briefly, a 96-well ELISA plate (442404, Thermo Scientific) was coated with 100  $\mu\text{L}$  per well of the capture antibody and incubated overnight at 4°C. After washing with 200  $\mu\text{L}$  of wash buffer (0.05% Tween 20 in PBS), the plate was blocked with 100  $\mu\text{L}$  of blocking buffer (1% bovine serum albumin in PBS) for 1 hour. After washing, 100  $\mu\text{L}$  of culture supernatant was added to each well and incubated for 2 hours at room temperature. Following another wash, 100  $\mu\text{L}$  of detection antibody was added to each well and incubated for 2 hours at room temperature. After a final wash, 100  $\mu\text{L}$  of the working dilution of streptavidin-HRP was added and incubated for 20 minutes at room temperature. The plate was washed again, and 100  $\mu\text{L}$  of substrate solution (NeA-Blue, Clinical Science Products, Inc., USA) was added and incubated for 20 minutes at room temperature. The reaction was stopped by adding 50  $\mu\text{L}$  of 1N HCl solution. Absorbance at 450 nm was determined using an ELISA microplate reader (SpectraMax M2, Molecular Devices, Inc).

## Mice

Eight- to twelve-week-old male C57BL/6 (B6) mice were obtained from the National Laboratory Animal Center (Taipei, Taiwan). The mice were housed under specific pathogen free conditions, and all animal studies were approved by the Animal Care and Use Committee of Chang Gung University (IACUC# CGU 105-027), according to the Guideline for the Care and Use of Laboratory Animals issued by the Council of Agriculture, Executive Yuan, Taiwan.

## In vivo Immune Responses to Formulated C34

Mice were injected intravenously with C34 (0.005 milligram per kilogram, MPK) or PLN-C34 (0.005 and 0.00125 MPK). After 2 hours, mouse sera were collected to determine serum IFN- $\gamma$ , IL-4, IL-2, GM-CSF, and G-CSF using the Beadlyte Mouse 6-plex Multi-Cytokine Detection System (Merck Millipore, Billerica, MA, US). Briefly, five microliters of mouse sera were diluted with 20  $\mu\text{L}$  assay buffer and added into each well of a 96-well black bottom plate (165305, Thermo Scientific). Twenty-five microliters of antibody-immobilized beads were added into each well and incubated overnight at 4°C. The plate was washed twice using plate washer for magnetic beads (ELx405, Bio-Tek) before adding 25  $\mu\text{L}$  of detection antibodies into each well and incubated with agitation on a plate shaker for 1 hour at room temperature. Then, 25  $\mu\text{L}$  of streptavidin-phycoerythrin was added into each well and incubated for additional 30 minutes at room temperature. After washing, the beads in each well were resuspended with 150  $\mu\text{L}$  of sheath fluid and mixed well on a plate shaker for 5 minutes. The cytokines on the beads were measured with a Luminex 200<sup>TM</sup> system (Merck Millipore, Billerica, MA, US).

## Flow Cytometry

Anti-CD3-FITC (145-2C11), anti-CD4-APC (RM4-5), anti-CD8-APC-Cy7 (53-3.7), anti-CD11b-APC (M1/70), anti-CD19-PE (6D5), anti-CD25-FITC (3C7), anti-NK1.1-PE-Cy7 (PK136), anti-Gr1-APC-Cy7 (RB6-8C5), and anti-FOXP3-PE (150D) antibodies were obtained from BioLegend (San Diego, CA, US).

Three days post glycolipid treatment, mouse splenocytes were obtained and counted using a Vi-Cell XR cell viability analyzer (Beckman Coulter, CA, US). Splenocyte subpopulations were identified via flow cytometry. For surface staining, splenocytes were resuspended in RPMI-1640 medium and incubated with antibodies for 30 minutes at 4°C. For intracellular staining, splenocytes were fixed with 450  $\mu\text{L}$  of FluoroFix buffer (#422101 BioLegend, San Diego, CA,

US) for 15 minutes at room temperature. After fixation, the splenocytes were washed three times with permeabilization wash buffer (#421002, BioLegend, San Diego, CA, US). A 100  $\mu$ L of permeabilization buffer containing anti-FOXP3-PE antibody was added and incubated with the cells for 30 minutes at 4°C. Following incubation, the cells were washed and resuspended in 500  $\mu$ L of PBS, then analyzed using a flow cytometry EC800 (SONY, Tokyo, Japan). EC800 software was utilized for data analysis. The gating strategies for immune cell subpopulations in spleen were defined as following: CD4<sup>+</sup> T (CD3<sup>+</sup>CD4<sup>+</sup>), CD8<sup>+</sup> T (CD3<sup>+</sup>CD8<sup>+</sup>), NK (CD3<sup>+</sup>NK1.1<sup>+</sup>), NKT (CD3<sup>+</sup>NK1.1<sup>+</sup>), B (CD19<sup>+</sup>), MDSC (CD11b<sup>+</sup>Gr1<sup>+</sup>), and Treg (CD4<sup>+</sup>CD25<sup>+</sup>FOXP3<sup>+</sup>) cells ([supplementary Figure 1](#)).

## Anti-Cancer Effect of PLN-C34 in vivo

C57BL/6 mice (n = 10/group) were intravenously injected with lung cancer TC-1 or melanoma B16F10 cells (10<sup>5</sup> cells/100  $\mu$ L PBS). One day after tumor injection, mice were injected intravenously with PBS, C34 (0.005 MPK), or PLN-C34 (0.005 and 0.00125 MPK) weekly for four weeks. The survival of these mice was analyzed by Kaplan-Meier cumulative plot.

## Immune Responses of Human Peripheral Blood Mononuclear Cells (PBMCs) to PLN-C34

PBMCs were isolated from heparinized whole blood using Ficoll-Paque PLUS (Cytiva, Massachusetts, US), seeded (10<sup>4</sup> cells/well) into each well of a 96-well plate, and cultured with 0.1  $\mu$ g/mL of C34 or PLN-C34 for 72 hours at 37°C. After being centrifuged at 400g for five minutes, the supernatant was collected to determine cytokines/chemokines by Beadlyte Human High Sensitivity T Cell Panel (Merck Millipore, Billerica, MA, US) as described in the above section. Human blood from healthy donors was obtained from Chang Gung Memorial Hospital (CGMH) at Linkou under the approval of the Institutional Review Board (IRB) at CGMH (IRB# 201700831A3).

## Statistical Analysis

The Shapiro–Wilk test and Levene test were used to verify the normal distribution and homogeneity of the data. Subsequently, the statistical significance between each group was analyzed by *t*-test. For groups with fewer than six samples, we used a permutation test with Benjamini & Hochberg correction to assess statistical significance. A P-value less than 0.05 was considered significant. The statistical significance of differences in survival time of tumor-bearing mice between each group was determined by the Log rank test.

## Results

### New Formulation PLN-C34 Stimulated Greater Immune Response at Lower Concentration Than C34 in vitro and in vivo

Finding an alternative to DMSO to maintain activity of hydrophobic C34 for clinical use is urgently needed. We evaluated the biological activities of C34 encapsulated in PEGylated lipid nanocarriers (PLN), which are designed for delivering hydrophobic agents. In vitro, mNK1.2 cells were stimulated with either C34 or PLN-C34 presented by A20-CD1d cells, and interleukin 2 (IL-2) secretion was measured. As shown in [Figure 1a](#), PLN-C34 induced significantly higher IL-2 secretion than C34 at three (unpaired *t*-test, *p* = 0.002) and six hours (unpaired *t*-test, *p* = 1.2e-6) post-stimulation. At 24 hours, the IL-2 levels in PLN-C34-treated cells were comparable to those in C34-treated cells. Notably, the EC<sub>50</sub> of PLN-C34 (0.004  $\mu$ g/mL) for inducing IL-2 production at 72 hours is ~4-fold lower than that of C34 (EC<sub>50</sub> = 0.017) ([Figure 1b](#)). These findings suggest that PLN-C34 may augment the NKT cell response compared to C34 dissolved in DMSO.

To delineate the immune modulatory activity of PLN-C34 in vivo, we analyzed cytokine induction and splenocyte sub-populations following the intravenous injection of mice with C34 (0.005 MPK) or PLN-C34 (0.005 and 0.00125 MPK). As shown in [Figure 1c](#), elevated levels of cytokines, including interferon  $\gamma$  (IFN- $\gamma$ ), interleukin 4 (IL-4), IL-2, granulocyte-macrophage colony-stimulating factor (GM-CSF), and granulocyte colony-stimulating factor (G-CSF), were detected in both the C34 and PLN-C34 groups, but were negligible in the control group two hours post-injection. The

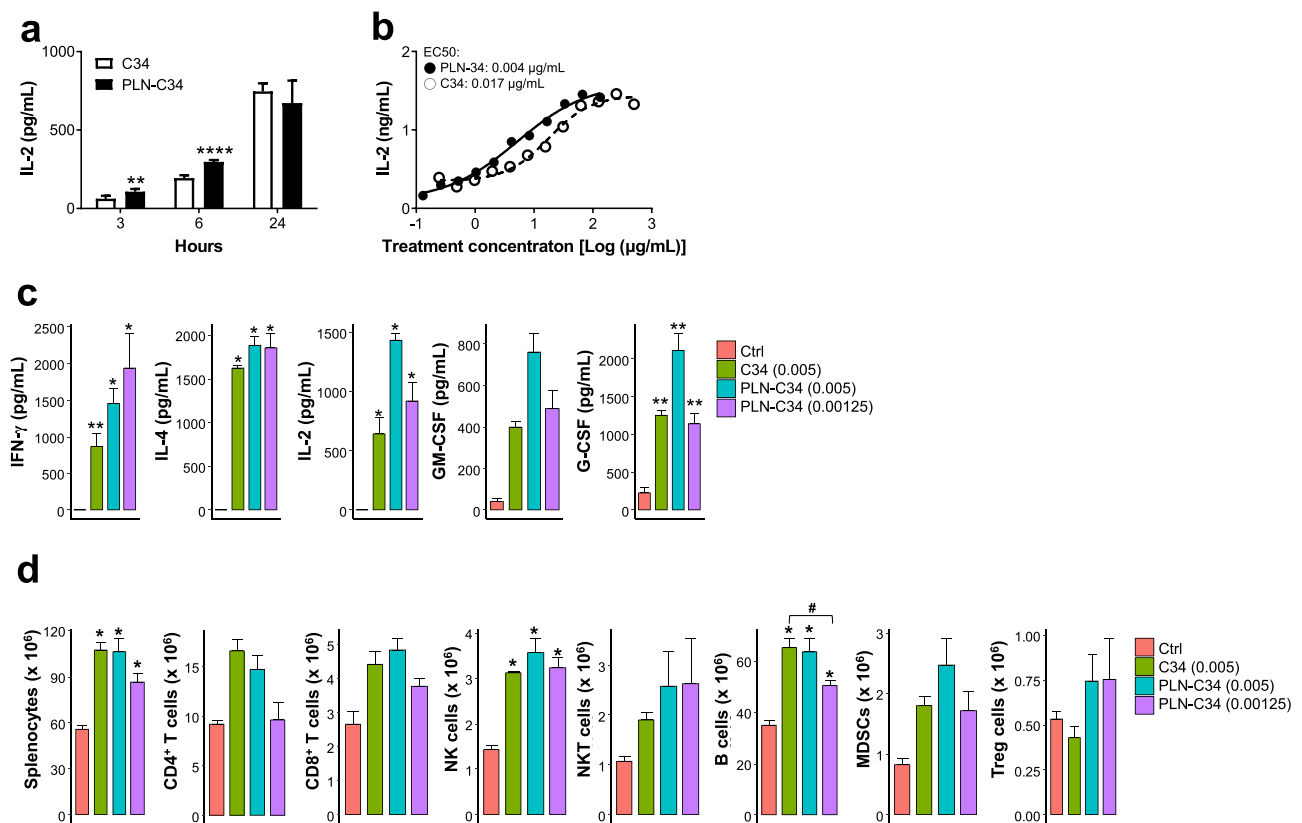


**Figure 1** PLN-C34 induced stronger immune responses than C34. **(a)** Murine NK1.2 cells were co-cultured with A20-CD1d cells in the presence of 1 µg/mL of C34 in DMSO (open column) or PLN-C34 (closed column). Supernatants were collected at 3 (n = 6/group), 6 (n = 6/group), and 24 (n = 3/group) hours after stimulation, and the concentration of mL-2 was determined by ELISA. \*\*  $p < 0.01$  and \*\*\*\*  $p < 0.0001$  by unpaired t-test. **(b)** Murine NK1.2 cells were co-cultured with A20-CD1d cells in the presence of C34 or PLN-C34 at various concentrations for 72 hours. Interleukin-2 concentrations in the supernatants were measured by ELISA. **(c)** C57BL/6 mice (n = 5/group) were i.v. injected with C34 (0.005 MPK) or PLN-C34 (0.005 and 0.00125 MPK). Mouse sera were collected at 2 hours after injection. Serum levels of IFN- $\gamma$ , IL-4, IL-2, GM-CSF, and G-CSF were analyzed using the Beadlyte mouse multi-cytokine detection system. **(d)** Three days after injection of C34 (0.005 MPK) or PLN-C34 (0.005 and 0.00125 MPK), subpopulations of splenocytes in the mice (n = 4/group) were determined by flow cytometry. Error bars represent the SEM. Ctrl: control, \*  $p < 0.05$  and \*\*  $p < 0.01$  vs control, #  $p < 0.05$  by permutation test with Benjamini & Hochberg correction.

C34 and PLN-C34 groups significantly stimulated the production of IFN- $\gamma$ , IL-4, IL-2, and G-CSF, in comparison to the control mice. Mice treated with PLN-C34 (0.005 MPK) exhibited higher levels of IL-2 ( $1431 \pm 61.6$  vs  $643.9 \pm 137.3$  pg/mL,  $p = 0.23$ ), GM-CSF ( $762.6 \pm 89$  vs  $397.5 \pm 30$  pg/mL,  $p = 0.34$ ), and G-CSF ( $2115.8 \pm 230.5$  vs  $1257 \pm 71$  pg/mL,  $p = 0.19$ ) compared to those treated with C34 (0.005 MPK); however, these differences were not statistically significant. Next, we analyzed the subpopulations of immune cells in the spleen three days after treatment with C34 (0.005 MPK) or PLN-C34 (0.00125 and 0.005 MPK). As shown in **Figure 1d**, the absolute number of splenocytes, NK cells, and B cells significantly increased in mice treated with C34 (0.005 MPK) or PLN-C34 (0.00125 or 0.005 MPK) compared to control mice. Although the numbers of CD4<sup>+</sup> T cells, CD8<sup>+</sup> T cells, NKT cells and MDSCs increased in mice treated with 0.005 MPK C34 (CD4<sup>+</sup> T:  $16.5 \pm 1.3 \times 10^6$ ,  $p = 0.07$ ; CD8<sup>+</sup> T:  $4.4 \pm 0.4 \times 10^6$ ,  $p = 0.07$ ; NKT:  $2.0 \pm 0.1 \times 10^6$ ,  $p = 0.1$ ; MDSC:  $1.8 \pm 0.2 \times 10^6$ ,  $p = 0.09$ ) or 0.005 MPK PLN-C34 (CD4<sup>+</sup> T:  $14.7 \pm 1.3 \times 10^6$ ,  $p = 0.07$ ; CD8<sup>+</sup> T:  $4.8 \pm 0.3 \times 10^6$ ,  $p = 0.07$ ; NKT:  $2.6 \pm 0.7 \times 10^6$ ,  $p = 0.2$ ; MDSC:  $2.5 \pm 0.5 \times 10^6$ ,  $p = 0.09$ ), this increase did not show a statistically significant difference from the control group (CD4<sup>+</sup> T:  $9.2 \pm 0.4 \times 10^6$ , CD8<sup>+</sup> T:  $2.7 \pm 0.4 \times 10^6$ , NKT:  $1.1 \pm 0.1 \times 10^6$ ; MDSC:  $0.8 \pm 0.1 \times 10^6$ ). There was no significant difference in the numbers of Treg cells among the mice in the C34 PLN-C34 (0.005 and 0.00125 MPK), or control groups. In general, we observed comparable potency between PLN-C34 and C34 in terms of cytokine production and lymphoid cell proliferation. Our findings show that PEGylated lipid nanocarriers preserve the NKT stimulatory activity of C34, supporting their potential to replace DMSO as a solvent.

## PLN-C34 Prolonged Survival of Tumor-Bearing Mice

We used the previously established syngeneic mouse tumor models, TC-1 lung cancer and B16F10 melanoma<sup>15</sup> to compare the efficacy of C34 in DMSO with that of water-soluble PLN-C34. One day after the intravenous injection of tumor cells, these mice were treated intravenously with C34 (0.005 MPK) or PLN-C34 (0.005 and 0.00125 MPK) weekly for four weeks. As shown in Figure 2, there was a significant prolongation of survival in TC-1-bearing mice treated with C34 (median survival: 34 days,  $p = 0.0024$ ) or PLN-C34 (0.005 MPK: 35 days,  $p = 0.0007$ ; 0.00125 MPK: 34.5 days,  $p = 0.0024$ ) compared to the control group (31.5 days). No significant difference in survival was observed among the groups treated with C34 (0.005 MPK) or PLN-C34 (0.005 and 0.00125 MPK). Similarly, in the B16F10 mouse model, prolonged survival was noted in the groups treated with C34 (30.5 days,  $p = 0.0139$ ) and PLN-C34 (0.005 MPK: 31.5 days,  $p = 0.0052$ ; 0.00125 MPK: 32 days,  $p = 0.0052$ ) compared to the control group (28.5 days). These findings indicate that the in vivo anticancer efficacy of PLN-C34 is comparable to that of C34 dissolved in DMSO.

## PLN-C34 Stimulated Comparable Cytokine Responses as C34 in Human PBMC

Finally, to investigate whether PLN-C34 could activate human NKT cells, we cultured human PBMC in the presence or absence of C34 or PLN-C34. Three days later, the culture supernatant was collected to determine the levels of GM-CSF, IFN- $\gamma$ , IL-2, and TNF- $\alpha$ . As shown in Figure 3, PLN-C34 induced comparable rises as C34 in the levels of following cytokines: GM-CSF ( $242 \pm 189.4$  vs  $163.3 \pm 81.8$  pg/mL,  $p = 0.5$ ), IFN- $\gamma$  ( $1000.3 \pm 921.0$  vs  $945 \pm 878.6$  pg/mL,  $p = 0.9$ ), IL-2 ( $589.7 \pm 408.4$  vs  $665.3 \pm 442.2$  pg/mL,  $p = 0.8$ ), and TNF- $\alpha$  ( $3273.7 \pm 3842.9$  vs  $1512 \pm 508.0$  pg/mL,  $p = 0.4$ ). These findings indicate that C34 in PEGylated lipid nanocarriers has comparable activity in stimulating human NKT cells to C34 dissolved in DMSO.

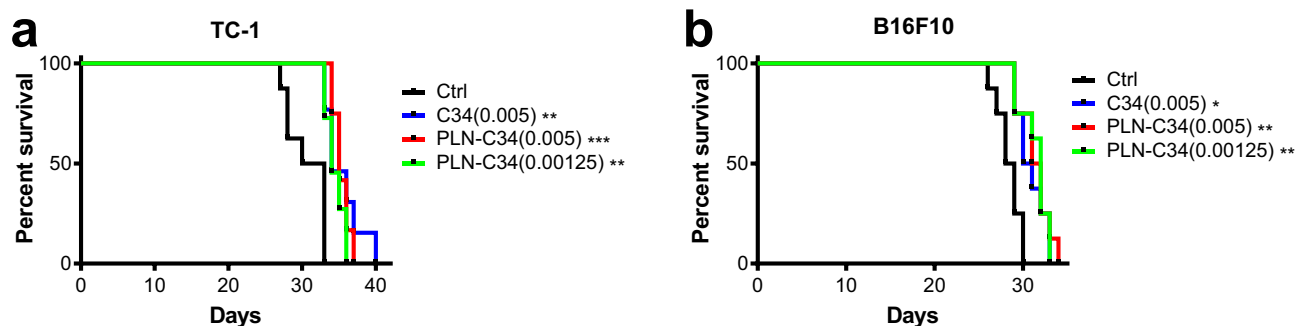


**Figure 2** Anti-cancer efficacy of PLN-C34 in tumor-bearing mice is comparable to C34. C57BL/6 mice ( $n = 8$  per group) were intravenously injected with either (a)  $10^5$  TC-1 lung cancer cells or (b) B16F10 melanoma cells. C34 (0.005 MPK) or PLN-C34 (0.005 and 0.00125 MPK) was administered intravenously on day 1, 8, 15, and 22. The survival of the mice was analyzed using Kaplan-Meier cumulative curve. \*  $p < 0.05$ , \*\*  $p < 0.01$  or \*\*\*  $p < 0.001$  compared with the control (Ctrl).

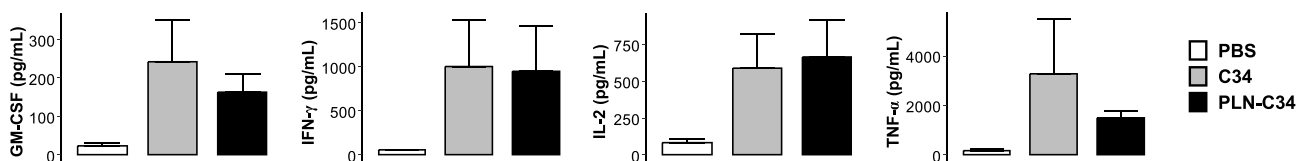


**Figure 3** PLN-C34 induced comparable cytokine responses in human PBMC as C34. Human PBMCs were cultured with  $1 \mu\text{g/mL}$  of C34 or PLN-C34 ( $n = 3/\text{group}$ ) for 72 hours. Afterward, the supernatants were collected, and the levels of GM-CSF, IFN- $\gamma$ , IL-2, and TNF- $\alpha$  were determined using beadlyte human multi-cytokine detection system.

## Discussion

To facilitate the clinical pharmaceutical applications, it is imperative to devise an optimal formulation for C34. While DMSO effectively dissolves hydrophobic glycolipid C34, systemic administration of DMSO is impractical. Several formulations for  $\alpha$ -GalCer glycolipid have been tested. One promising approach involved encapsulating  $\alpha$ -GalCer and insulin B peptide in a liposome composed of 1,2-dioleoyl-sn-glycero-3-phosphocholine, 1,2-dioleoyl-sn-glycero-3-phosphoglycerol, and Cholesterol. The  $\alpha$ -GalCer-insulin B peptide liposomes demonstrated a promising effect on the suppression of the onset of type 1 diabetes in NOD mice.<sup>28</sup> Another formulation, a liposome containing  $\alpha$ -GalCer combined with palmitoylated tumor antigen and palmitoylated LeY, increased uptake by monocyte-derived dendritic cells.<sup>29</sup> However, these formulations of hydrophobic glycolipids are still in the preclinical phase and are not yet accessible for clinical application.

C34 is a synthetic analog of  $\alpha$ -galactosylceramide ( $\alpha$ -GalCer). Pharmacokinetic studies of  $\alpha$ -GalCer (administered at doses ranging from 50 to 4800  $\mu\text{g}/\text{m}^2$ ) in a formulation containing sucrose, L-histidine, and polysorbate 20 indicated no evidence of drug accumulation or saturation.<sup>12</sup> When administered at a dosage of 4800  $\mu\text{g}/\text{m}^2$ ,  $\alpha$ -GalCer exhibits a half-life of approximately 64 hours, with a clearance rate of 0.18 liters per hour. The pharmacokinetics of PLN-C34 is likely to be comparable to those of  $\alpha$ -GalCer.

The  $\alpha$ -galactosylceramide analogs display the ability to expand NKT cells in vitro, suggesting that they are not cytotoxic.<sup>30</sup> Additionally, the PLN is composed of DSPE-PEG, which is an FDA-approved phospholipids-polymer conjugate for drug delivery. Such formulation is known for its biocompatibility, biodegradability, and non-toxicity.<sup>31</sup>

Encapsulation with micelles facilitates the solubility of water-insoluble drugs in aqueous solution due to the affinity between these drugs and hydrophobic solvent.<sup>32</sup> This approach may offer a promising avenue for increasing the bioavailability of those compounds with inherent solubility challenges. Additionally, modifying biological molecules through covalent conjugation with polyethylene glycol (PEG) improves their solubility and stability. PEGylated polymeric micelles, which are soluble lipid-based nanocarriers, have been designed to enhance the aqueous solubility of poorly soluble compounds, protect them from degradation, and improve their availability at disease sites.<sup>26,27,33</sup> Furthermore, PEGylated polymeric micelle-encapsulated drugs have been shown to accumulate within tumor sites through the enhanced permeability and retention effect.<sup>34</sup> Consequently, PLN might form PEGylated polymeric micelles to enhance the solubility of glycolipid C34.

Several PEGylated hormones and cytokines have been approved by the FDA and have reached the market.<sup>25</sup> PEGylated liposomal doxorubicin HCl (Doxil) was the first FDA-approved nano-drug for ovarian cancer and sarcomas.<sup>35</sup> Additionally, when formulated into DSPE-PEG2000 micelles, Ridaforolimus, a highly lipophilic compound, demonstrated an prolonged half-life.<sup>36</sup> So far, most of the FDA-approved PEGylated entities are small molecules, peptide, and protein. Our results demonstrate that PEGylated lipid nanocarriers could be an ideal formulation for glycolipids.

PEGylated compounds may show decreased uptake by numerous cell lines. The reduced cellular uptake is attributed to the hydrophilic nature and nanoparticle shielding properties of PEG.<sup>37–39</sup> Additionally, evidence suggests that endosomal transfer of PEGylated compounds occurs.<sup>40</sup> Interestingly,  $\alpha$ -GalCer, as well as C34, is processed and loaded onto CD1d at the late endosome/lysosome, and then  $\alpha$ -GalCer-CD1d complexes are transported to the cell surface to activate NKT cells.<sup>41,42</sup> This might elucidate why PEGylated lipid nanocarriers did not interfere the presentation process of C34 to CD1d molecules; conversely, PLN-C34 can effectively stimulate NKT cells to secrete comparable amounts of cytokines as C34, including IFN- $\gamma$ , IL-4, IL-2, and G-CSF.

PEGylation has been shown to improve the uptake of particles by dendritic cells. When PEGylated particles were administered subcutaneously, they accumulated in the draining lymph nodes, where the dendritic cells uptake the particles, thereby enhancing a robust immune response.<sup>43</sup> For example, the incorporation of PEG into the lipopeptide R<sub>4</sub>Pam<sub>2</sub>Cys has been shown to induce maturation of dendritic cells, which in turn activates T cells.<sup>44</sup> In this study, our findings demonstrate that PLN-C34 could enhance cytokine production in vivo, which may be attributed to the activation of NKT cells by dendritic cells presenting C34.

## Conclusion

Our study here demonstrated a non-liposomal PEGylated lipid nanocarrier formulation that improved the water solubility of hydrophobic C34. PLN-C34 exhibited potent bioactivities in activating murine and human NKT cells in vitro. Importantly, the in vivo anti-cancer efficacy of C34 was not compromised by the formulation. Thus, this PEGylated lipid nanocarrier offers an ideal strategy to replace DMSO for the formulation of C34.

## Data Sharing Statement

The datasets for this study are available on request to the corresponding author.

## Ethics Approval and Informed Consent

All animal studies were approved by Animal Care and Use Committee of Chang Gung University (IACUC# CGU 105-027). Human blood from healthy donor was obtained in Chang Gung Memorial Hospital (CGMH) at Linkou under the approval of the Institutional Review Board (IRB) at CGMH (IRB# 201700831A3). Written informed consent was obtained from the donors.

## Consent for Publication

The authors affirm that human research participants provided informed consent for publication of the data in [Figure 3](#).

## Acknowledgments

We sincerely thank Dr. Tsuimin Tsai and OPKO Company for providing C34 and PLN-C34.

## Author Contributions

All authors made a significant contribution to the work reported, whether that is in the conception, study design, execution, acquisition of data, analysis and interpretation, or in all these areas; took part in drafting, revising or critically reviewing the article; gave final approval of the version to be published; have agreed on the journal to which the article has been submitted; and agree to be accountable for all aspects of the work.

## Funding

This work was supported by National Science and Technology Council (NSTC113-2321-B-182-004 and NSTC113-2314-B-182A-012) and Chang Gung Medical Foundation (CMRPG3N0181-2, CMRPG3K0311, and OMRPG3C0018).

## Disclosure

Prof. Alice L. Yu is one of the inventors of C34; In addition, Prof. Alice Yu has a patent for C34 licensed to RuenHui Biopharmaceuticals. Other authors have no relevant financial or non-financial interests to disclose.

## References

1. Jeong D, Woo YD, Chung DH. Invariant natural killer T cells in lung diseases. *Exp Mol Med*. 2023;55(9):1885–1894. doi:10.1038/s12276-023-01024-x
2. Tsuji M, Nair MS, Masuda K, et al. An immunostimulatory glycolipid that blocks SARS-CoV-2, RSV, and influenza infections in vivo. *Nat Commun*. 2023;14(1):3959. doi:10.1038/s41467-023-39738-1
3. Choi Y, Saron WA, O'Neill A, et al. NKT cells promote Th1 immune bias to dengue virus that governs long-term protective antibody dynamics. *J Clin Invest*. 2024;134(18). doi:10.1172/JCI1169251.
4. Choi J, Mele TS, Porcelli SA, Savage PB, Haeryfar SMM. Harnessing the versatility of invariant NKT cells in a stepwise approach to sepsis immunotherapy. *J Immunol*. 2021;206(2):386–397. doi:10.4049/jimmunol.2000220
5. Wu TN, Hung JT, Hung TH, Wang YH, Wu JC, Yu AL. Effective suppression of tumor growth and hepatic metastasis of neuroblastoma by NKT-stimulatory phenyl glycolipid. *Biomed Pharmacother*. 2024;177:117040. doi:10.1016/j.biopha.2024.117040
6. Hung JT, Tsai YC, Lin WD, et al. Potent adjuvant effects of novel NKT stimulatory glycolipids on hemagglutinin based DNA vaccine for H5N1 influenza virus. *Antiviral Res*. 2014;107:110–118. doi:10.1016/j.antiviral.2014.04.007
7. Luo T, Tan X, Qing G, Yu J, Liang XJ, Liang P. A natural killer T cell nanoagonist-initiated immune cascade for hepatocellular carcinoma synergistic immunotherapy. *Nanoscale*. 2024;16(23):11126–11137. doi:10.1039/D4NR00847B



8. Lang GA, Shrestha B, Amadou Amani S, Shadid TM, Ballard JD, Lang ML. alpha-galactosylceramide-reactive NKT cells increase IgG1 class switch against a clostridioides difficile polysaccharide antigen and enhance immunity against a live pathogen challenge. *Infect Immun.* 2021;89(11): e0043821. doi:10.1128/IAI.00438-21
9. Umeshappa CS, Sole P, Yamanouchi J, et al. Re-programming mouse liver-resident invariant natural killer T cells for suppressing hepatic and diabetogenic autoimmunity. *Nat Commun.* 2022;13(1):3279. doi:10.1038/s41467-022-30759-w
10. Huang JR, Tsai YC, Chang YJ, et al. alpha-Galactosylceramide but not phenyl-glycolipids induced NKT cell anergy and IL-33-mediated myeloid-derived suppressor cell accumulation via upregulation of egr2/3. *J Immunol.* 2014;192(4):1972–1981. doi:10.4049/jimmunol.1302623
11. van der Vliet HJ, Molling JW, von Blomberg BM, et al. The immunoregulatory role of CD1d-restricted natural killer T cells in disease. *Clin Immunol.* 2004;112(1):8–23. doi:10.1016/j.clim.2004.03.003
12. Giaccone G, Punt CJ, Ando Y, et al. A Phase I study of the natural killer T-cell ligand alpha-galactosylceramide (KRN7000) in patients with solid tumors. *Clin Cancer Res.* 2002;8(12):3702–3709.
13. Dhodapkar MV, Geller MD, Chang DH, et al. A reversible defect in natural killer T cell function characterizes the progression of premalignant to malignant multiple myeloma. *J Exp Med.* 2003;197(12):1667–1676. doi:10.1084/jem.20021650
14. Chen YN, Hung JT, Jan FD, et al. Diversity-oriented synthesis of a molecular library of immunomodulatory alpha-galactosylceramides with fluorine-tag-assisted purification and evaluation of their bioactivities in regard to IL-2 secretion. *Int J Mol Sci.* 2022;23(21): 13403. doi:10.3390/ijms232113403
15. Wu T-N, Lin K-H, Chang Y-J, et al. Avidity of CD1d-ligand-receptor ternary complex contributes to T-helper 1 (Th1) polarization and anticancer efficacy. *Proc Natl Acad Sci.* 2011;108(42):17275–17280. doi:10.1073/pnas.1114255108
16. Wen Y, Ding D, Luo MQ, et al. Rationally designed highly potent NKT cell agonists with different cytokine selectivity through hydrogen-bond interaction. *J Med Chem.* 2024;67(15):12819–12834. doi:10.1021/acs.jmedchem.4c00782
17. Hoya M, Nagamatsu T, Fujii T, et al. Impact of Th1/Th2 cytokine polarity induced by invariant NKT cells on the incidence of pregnancy loss in mice. *Am J Reproductive Immunol.* 2018;79(3): e12813. doi:10.1111/aji.12813
18. Hung J-T, Sawant RC, Wang S-H, et al. Structure-based design of NH-modified alpha-galactosyl ceramide (KRN7000) analogues and their biological activities. *ChemistrySelect.* 2016;1(15):4564–4569. doi:10.1002/slct.201600854
19. Kang M-H, Das J, Gurunathan S, et al. The cytotoxic effects of dimethyl sulfoxide in mouse preimplantation embryos: a mechanistic study. *Theranostics.* 2017;7(19):4735–4752. doi:10.7150/thno.21662
20. Galvao J, Davis B, Tilley M, Normando E, Duchon MR, Cordeiro MF. Unexpected low-dose toxicity of the universal solvent DMSO. *FASEB J.* 2014;28(3):1317–1330. doi:10.1096/fj.13-235440
21. Sheikhpour M, Barani L, Kasaeian A. Biomimetics in drug delivery systems: a critical review. *J Controlled Release.* 2017;253:97–109. doi:10.1016/j.jconrel.2017.03.026
22. Isoglu IA, Ozsoy Y, Isoglu SD. Advances in micelle-based drug delivery: cross-linked systems. *Curr. Top. Med. Chem.* 2017;17(13):1469–1489. doi:10.2174/1568026616666161222110600
23. Farhoudi L, Maryam Hosseinikhah S, Vahdat-Lasemi F, Sukhorukov VN, Kesharwani P, Sahebkar A. Polymeric micelles paving the way: recent breakthroughs in camptothecin delivery for enhanced chemotherapy. *Int J Pharm.* 2024;659:124292. doi:10.1016/j.ijpharm.2024.124292
24. Krishnan J, Poomalai P, Ravichandran A, Reddy A, Sureshkumar R. A concise review on effect of PEGylation on the properties of lipid-based nanoparticles. *Assay Drug Dev Technol.* 2024;22(5):246–264. doi:10.1089/adt.2024.015
25. Gao Y, Joshi M, Zhao Z, Mitragotri S. PEGylated therapeutics in the clinic. *Bioeng Transl Med.* 2024;9(1):e10600. doi:10.1002/btm2.10600
26. Suk JS, Xu Q, Kim N, Hanes J, Ensign LM. PEGylation as a strategy for improving nanoparticle-based drug and gene delivery. *Adv. Drug Delivery Rev.* 2016;99(Pt A):28–51. doi:10.1016/j.addr.2015.09.012
27. Vukovic L, Khatib FA, Drake SP, et al. Structure and dynamics of highly PEG-ylated sterically stabilized micelles in aqueous media. *J Am Chem Soc.* 2011;133(34):13481–13488. doi:10.1021/ja204043b
28. Akimoto H, Fukuda-Kawaguchi E, Duramad O, Ishii Y, Tanabe K. A novel liposome formulation carrying both an insulin peptide and a ligand for invariant natural killer T cells induces accumulation of regulatory T cells to islets in nonobese diabetic mice. *J Diabet Res.* 2019;2019:1–9. doi:10.1155/2019/9430473
29. Stolk DA, de Haas A, Vree J, et al. Lipo-based vaccines as an approach to target dendritic cells for induction of T- and iNKT cell responses. *Front Immunol.* 2020;11:990. doi:10.3389/fimmu.2020.00990
30. Chang YJ, Huang JR, Tsai YC, et al. Potent immune-modulating and anticancer effects of NKT cell stimulatory glycolipids. *Proc Natl Acad Sci U S A.* 2007;104(25):10299–10304. doi:10.1073/pnas.0703824104
31. Kowalska M, Broniatowski M, Mach M, Plachta Ł, Wydro P. The effect of the polyethylene glycol chain length of a lipopolymer (DSPE-PEGn) on the properties of DPPC monolayers and bilayers. *J Mol Liq.* 2021;335:116529. doi:10.1016/j.molliq.2021.116529
32. Kalepu S, Nekkanti V. Insoluble drug delivery strategies: review of recent advances and business prospects. *Acta Pharmaceutica Sinica B.* 2015;5(5):442–453. doi:10.1016/j.apsb.2015.07.003
33. Al-Amili M, Jin Z, Wang Z, Guo S. Self-assembled micelles of amphiphilic PEGylated drugs for cancer treatment. *Curr Drug Targets.* 2021;22(8):870–881. doi:10.2174/1389450122666201231130702
34. Takakura Y, Takahashi Y. Strategies for persistent retention of macromolecules and nanoparticles in the blood circulation. *J Control Release.* 2022;350:486–493. doi:10.1016/j.jconrel.2022.05.063
35. O'Brien MER, Wigler N, Inbar M, et al. Reduced cardiotoxicity and comparable efficacy in a phase III trial of pegylated liposomal doxorubicin HCl (CAELYX™/Doxil) versus conventional doxorubicin for first-line treatment of metastatic breast cancer. *Ann Oncol.* 2004;15(3):440–449. doi:10.1093/annonc/mdh097
36. Remsberg C, Zhao Y, Takemoto J, Bertram R, Davies N, Forrest M. Pharmacokinetic evaluation of a DSPE-PEG2000 micellar formulation of ridaforolimus in rat. *Pharmaceutics.* 2012;5(4):81–93. doi:10.3390/pharmaceutics5010081
37. Gaikwad H, Wang G, Li Y, Bourne D, Simberg D. Surface modification of erythrocytes with lipid anchors: structure-activity relationship for optimal membrane incorporation, in vivo retention, and immunocompatibility. *Adv Nanobiomed Res.* 2022;2(8). doi:10.1002/anbr.202270081
38. Cruje C, Chithrani D. Polyethylene glycol density and length affects nanoparticle uptake by cancer cells. *J Nanomed Res.* 2014;1(00006):8. doi:10.15406/jnmr.2014.01.00006

39. Dabkowska M, Luczkowska K, Roginska D, et al. Novel design of (PEG-ylated)PAMAM-based nanoparticles for sustained delivery of BDNF to neurotoxin-injured differentiated neuroblastoma cells. *J Nanobiotechnology*. 2020;18(1):120. doi:10.1186/s12951-020-00673-8
40. Remaut K, Lucas B, Braeckmans K, Demeester J, De Smedt SC. Pegylation of liposomes favours the endosomal degradation of the delivered phosphodiester oligonucleotides. *J Control Release*. 2007;117(2):256–266. doi:10.1016/j.jconrel.2006.10.029
41. Roberts TJ, Sriram V, Spence PM, et al. Recycling CD1d1 molecules present endogenous antigens processed in an endocytic compartment to NKT cells. *J Immunol*. 2002;168(11):5409–5414. doi:10.4049/jimmunol.168.11.5409
42. Ly D, Moody DB. The CD1 size problem: lipid antigens, ligands, and scaffolds. Cellular and molecular life sciences. *CMLS*. 2014;71(16):3069–3079. doi:10.1007/s00018-014-1603-6
43. Zhan X, Tran KK, Shen H. Effect of the poly(ethylene glycol) (PEG) density on the access and uptake of particles by antigen-presenting cells (APCs) after subcutaneous administration. *Mol Pharm*. 2012;9(12):3442–3451. doi:10.1021/mp300190g
44. Sekiya T, Yamagishi J, Gray JHV, et al. PEGylation of a TLR2-agonist-based vaccine delivery system improves antigen trafficking and the magnitude of ensuing antibody and CD8(+) T cell responses. *Biomaterials*. 2017;137:61–72. doi:10.1016/j.biomaterials.2017.05.018

## Drug Design, Development and Therapy

Dovepress

### Publish your work in this journal

Drug Design, Development and Therapy is an international, peer-reviewed open-access journal that spans the spectrum of drug design and development through to clinical applications. Clinical outcomes, patient safety, and programs for the development and effective, safe, and sustained use of medicines are a feature of the journal, which has also been accepted for indexing on PubMed Central. The manuscript management system is completely online and includes a very quick and fair peer-review system, which is all easy to use. Visit <http://www.dovepress.com/testimonials.php> to read real quotes from published authors.

Submit your manuscript here: <https://www.dovepress.com/drug-design-development-and-therapy-journal>